

# Boron Isotope Effect in Superconducting $\text{MgB}_2$ .

S. L. Bud'ko, G. Lapertot\*, C. Petrovic, C. E. Cunningham†, N. Anderson, and P. C. Canfield  
*Ames Laboratory and Department of Physics and Astronomy Iowa State University, Ames, IA 50011*  
(October 3, 2018)

We report the preparation method of, and boron isotope effect for  $\text{MgB}_2$ , a new binary intermetallic superconductor with a remarkably high superconducting transition temperature  $T_c(^{10}\text{B}) = 40.2$  K. Measurements of both temperature dependent magnetization and specific heat reveal a 1.0 K shift in  $T_c$  between  $\text{Mg}^{11}\text{B}_2$  and  $\text{Mg}^{10}\text{B}_2$ . Whereas such a high transition temperature might imply exotic coupling mechanisms, the boron isotope effect in  $\text{MgB}_2$  is consistent with the material being a phonon-mediated BCS superconductor.

PACS numbers: 74.70.Ad, 74.62.Bf

The discovery of superconductivity with  $T_c \approx 39$  K in magnesium diboride ( $\text{MgB}_2$ ) was announced in January 2001<sup>1</sup>. It caused excitement in the solid state physics community because it introduced a new, simple (3 atoms per unit cell) binary intermetallic superconductor with a record high (by almost a factor of two) superconducting transition temperature for a non-oxide and non- $\text{C}_{60}$ -based compound. The reported value of  $T_c$  seems to be either above or at the limit suggested theoretically several decades ago for BCS, phonon-mediated superconductivity<sup>2,3</sup>. An immediate question raised by this discovery is whether this remarkably high  $T_c$  is due to some form of exotic coupling. Therefore, any experimental data that can shed light on the mechanism of superconductivity in this material are of keen interest.

One probe of the extent to which phonons mediate superconductivity is the isotope effect<sup>4,5</sup>. In the classical form of BCS theory<sup>6</sup>, the isotope coefficient  $\alpha$ , defined by the relation  $T_c \propto M^{-\alpha}$ , where  $M$  is the mass of the element, is equal to 1/2. For simple metals like Hg, Pb, Sn, and Zn, the isotope coefficient is found experimentally to be close to 1/2. More detailed and realistic theories predict slight deviations from  $\alpha = 1/2$ <sup>7</sup>. In this Letter, we describe how to prepare high-quality powders of  $\text{MgB}_2$  and, more importantly, present data on the boron isotope effect, which is consistent with phonon mediated coupling within the framework of the BCS model.

$\text{MgB}_2$  crystallizes in the hexagonal  $\text{AlB}_2$  type structure, which consists of alternating hexagonal layers of Mg atoms and graphite-like honeycomb layers of B atoms.

This material, along with other  $3d - 5d$  transition metal diborides, has been studied for several decades, mainly as a promising technological material<sup>8</sup>. The B - Mg binary phase diagram<sup>9</sup> is shown in Fig. 1. As can be seen,  $\text{MgB}_2$  decomposes peritectically and has no exposed liquid-solidus line. Whereas the growth of single crystals of this compound promises to be a difficult problem, high quality powders can be formed in the following manner. Elemental Mg (99.9 % pure in lump form) and isotopically pure boron (99.5 % pure, < 100 mesh) are combined in a sealed Ta tube in a stoichiometric ratio. The Ta tube is then sealed in a quartz ampoule, placed in a 950° C box furnace for two hours, and then removed and allowed to cool to room temperature. The quartz ampoule and the Ta tubing are not attacked, but there is a distinct bowing out of the Ta tube where the  $\text{MgB}_2$  powders form. The height of this bowing scales with the height of the  $\text{MgB}_2$  powders and seems to be associated with an expansion of the B powder as the  $\text{MgB}_2$  forms, rather than a Mg vapor pressure (which would bow out the tube over its whole length). It should be noted that if larger pieces of B are used, then this reaction scheme does not produce homogeneous material. This, combined with the phase diagram shown in Fig. 1, implies that, at least to some extent, the reaction takes place via the diffusion of Mg into the B particles.

The powder X-ray diffraction pattern of the  $\text{Mg}^{10}\text{B}_2$  powder is shown in Fig. 2 with the peaks indexed to the hexagonal unit cell of  $\text{MgB}_2$ . From Fig. 2 the unit cell lattice parameters for  $\text{Mg}^{10}\text{B}_2$  are  $a = 3.1432 \pm 0.0315$  and  $c = 3.5193 \pm 0.0323$  Å.

The temperature dependent magnetization of the samples was measured in a Quantum Design MPMS-7 SQUID magnetometer in an applied field of 25 G. An onset criterion of 2% of the full, low temperature diamagnetic signal was used to determine  $T_c$  from the zero-field-cooled  $M(T)$  data that were taken on warming. In this letter we report measurements on four types of samples with the following morphologies:  $\text{Mg}^{10}\text{B}_2$ ,  $\text{Mg}^{11}\text{B}_2$  and  $\text{Mg}^{10}\text{B}^{11}\text{B}$  were all solid pieces of sample cut from the pellet that formed in the Ta reaction tubes whereas, the commercial sample was a fine powder. The three solid, isotopic samples each had  $M/H > 150\%$  of  $-1/4\pi$  at low temperature and the powder sample had  $M/H > 200\%$  of  $-1/4\pi$ . By assuming spherical or slightly plate-like grains both of these values are consistent with demagnetization effects and 100% diamagnetism. The plotted magnetization data are all normalized to 1 at low temperatures for easier comparison. The specific heat data were taken using the heat capacity option of a Quantum

\*On leave from Commissariat à l'Energie Atomique, DRFMC-SPSMS, 38054 Grenoble, France

†On leave from Dept. of Physics, Grinnell College, Grinnell, IA 50112

Design PPMS-9 system in zero and 90 kG applied field.

The magnetization curves of a commercial (Alfa-Aesar 98% pure)  $\text{MgB}_2$  powder and prepared  $\text{Mg}^{11}\text{B}_2$  material are shown in Fig. 3. The commercial powder has a lower  $T_c$  (37.5 K) and a broader superconducting transition. At present, it is not clear what causes the suppression of  $T_c$ , but the difference may be due to impurities present in the material<sup>10</sup>.

Figure 4a presents the temperature-dependent magnetization of  $\text{Mg}^{10}\text{B}_2$  and  $\text{Mg}^{11}\text{B}_2$ . There is a clear separation between the data of  $\text{Mg}^{10}\text{B}_2$  and  $\text{Mg}^{11}\text{B}_2$ . Using the 2% onset of diamagnetism criterion mentioned above, the superconducting transition temperatures are 39.2K for  $\text{Mg}^{11}\text{B}_2$  and 40.2K for  $\text{Mg}^{10}\text{B}_2$ . The widths of the transitions (90% – 10%) are 0.4 K and 0.5 K for  $\text{Mg}^{11}\text{B}_2$  and  $\text{Mg}^{10}\text{B}_2$ , respectively.

In Fig. 5 the temperature-dependent specific heat data for  $\text{Mg}^{10}\text{B}_2$  and  $\text{Mg}^{11}\text{B}_2$  in zero and 90 kG applied field are shown. Whereas the data were collected between 2 K and 50 K, Fig. 5 presents a more limited temperature range to clearly show the shift in  $T_c$  associated with the isotope effect. The transitions are shifted by the same 1.0 K seen in Fig. 4a. Due to the temperature of the superconducting transition and the porous nature of the samples it is difficult to extract precise values of the Debye temperature and the linear coefficient of the specific heat from these data, but we can estimate  $\Theta_D = 750 \pm 30$  K and  $\gamma = 3 \pm 1$  mJ/mol K<sup>2</sup>. This leads to values of  $\Delta C_p/\gamma T_c$  near unity. The primary point of these data should not be lost though: a clear isotope shift in  $T_c$  can be seen in both magnetization and specific heat data.

To understand this substantial shift in  $T_c$ , it should be noted that if  $T_c$  is assumed to scale with the square root of the formula unit mass, then the shift in  $T_c$  would be expected to be 0.87 K. On the other hand, if  $T_c$  is assumed to scale with the square root of just the boron mass (i.e. the  $T_c$  is mediated solely by boron vibrations), then the shift in  $T_c$  would be 1.9 K. These two values of  $\Delta T_c$  provide a caliper of the size of the isotope effect within the simplest BCS framework. Viewed in this light, the shift in  $T_c$  of 1.0 K implies that the phonon modes mediating the superconductivity are somewhat weighted toward being boron-like in character.

More formally, we can estimate the partial (boron) isotope exponent  $\alpha_B$  in this compound via  $\alpha_B = -\Delta \ln T_c / \Delta \ln M_B$ <sup>4,5</sup>. From the measured values of  $T_c$ , the boron isotope exponent can be estimated as  $\alpha_B = 0.26 \pm 0.03$ . It is worth mentioning that this value is close to the boron isotope exponents obtained for the  $\text{YNi}_2\text{B}_2\text{C}$  and  $\text{LuNi}_2\text{B}_2\text{C}$  borocarbides,<sup>11,12</sup> where theoretical work<sup>13</sup> suggested that the phonons responsible for the superconductivity are high-frequency boron  $A_{1g}$  optical modes. Early band-structure calculations<sup>14</sup> suggested substantial electron transfer from the magnesium atom to the two boron atoms in the unit cell. Recent band structure work<sup>15</sup> suggests that the superconductivity in  $\text{MgB}_2$  is essentially due to the metallic nature of the boron sheets.

Figure 4b presents data on a 50-50 mixture of boron isotopes:  $\text{Mg}^{10}\text{B}^{11}\text{B}$ . Also shown is the normalized sum of the pure  $\text{Mg}^{10}\text{B}_2$  and  $\text{Mg}^{11}\text{B}_2$  magnetization data shown in Fig. 4a. Given that the starting materials were a lump of Mg and grains of  $^{10}\text{B}$  and  $^{11}\text{B}$ , if there were no mixing between the boron particles as the  $\text{MgB}_2$  was formed then one might expect the data to look like the sum plot, i.e. separate grains of  $\text{Mg}^{10}\text{B}_2$  and  $\text{Mg}^{11}\text{B}_2$  acting independently. As can be seen, the  $\text{Mg}^{10}\text{B}^{11}\text{B}$  data does not show two steps and manifests a significantly broadened transition. Using the 2% criterion,  $T_c = 39.9$  K but, more significantly, the width of the transition is 2.1 K, a factor of four broader than either of the isotopically pure samples. It should be noted that the  $\text{Mg}^{10}\text{B}^{11}\text{B}$  sample was made from exactly the same starting chemicals, via the same technique, and had the same morphology (a sintered lump) as the two isotopically pure samples. The origin of this broadening is not as of yet clear, but it may hint that the effect of isotopic disorder on the boron phonon modes plays a significant role.

In conclusion, a significant boron isotope effect ( $\Delta T_c = 1.0$  K, partial isotope exponent  $\alpha_B \approx 0.26$ ) was observed in  $\text{MgB}_2$ . This shift is clearly seen in both magnetization and specific heat measurements. This observation is consistent with a phonon mediated BCS superconducting mechanism in this compound and with the possibility that boron phonon modes are playing an important role.

We

appreciate useful discussions with Doug Finnemore, R. W. McCallum, K. Dennis and V. Antropov. Ames Laboratory is operated for the US Department of Energy by Iowa State University under Contract No. W-7405-Eng-82. This work was supported by the Director for Energy Research, Office of Basic Energy Sciences.

- 
- <sup>1</sup> J. Akimitsu, Symposium on Transition Metal Oxides. Sendai, January 10, 2001; J.Nagamatsu, N.Nakagawa, T.Muranaka, Y.Zenitani, and J.Akimitsu, unpublished.
  - <sup>2</sup> W. L. McMillan, Phys. Rev. **167**, 331 (1968).
  - <sup>3</sup> see for example E. G. Maksimov in: Superconductivity, Proc. P. N. Lebedev Institute v. 86, ed. N. G. Basov (Consultants Bureau, NY, London, 1977) p.105.
  - <sup>4</sup> J. P. Franck in: Physical Properties of High Temperature Superconductors IV, ed. D. M. Ginsberg (World Scientific, Singapore, 1994) p.189.
  - <sup>5</sup> R. Kishore in: Studies of High Temperature Superconductors Volume 29, ed. A. Narlikar (Nova Science Publishers, Commack, NY, 1999) p.23.
  - <sup>6</sup> J. Bardeen, L. N. Cooper, and J. R. Schrieffer, Phys. Rev. **108**, 1175 (1957).
  - <sup>7</sup> for review see: J. P. Carbotte, Rev. Mod. Phys. **62**, 1027 (1990).

- <sup>8</sup> see for example: B. Aronsson, T. Lundstrom, and S. Rundquist, Borides, Silicides and Phosphides (Methuen, London, 1965); J. L. Hoard, and R. E. Hughes, The Chemistry of Boron and Its Compounds (J. Wiley, NY, 1967).
- <sup>9</sup> Binary Alloy Phase Diagrams, Second Edition, Edited by T. Massalski, (A.S.M International, 1990).
- <sup>10</sup> Alfa Aesar, A Johnson Matthey Company, stock # 88149: Magnesium boride, 98% (assay)  $\text{MgB}_2$  (possible impurities are not specified). It should be noted that the powder X-ray diffraction ( $\text{Cu K}\alpha$  radiation) on this sample shows an extra unidentified peak at  $2\theta \approx 15.4^\circ$ .
- <sup>11</sup> D. D. Lawrie, and J. P. Franck, Physica C, **245**, 159 (1995).
- <sup>12</sup> K. O. Cheon, I. R. Fisher, and P. C. Canfield, Physica C, **312**, 35 (1999).
- <sup>13</sup> L. F. Mattheiss, T. Siegrist, and R. J. Cava, Solid State Commun. **91**, 587 (1994).
- <sup>14</sup> D. R. Armstrong, and P. G. Perkins, J. Chem. Soc., Faraday Trans. 2, **75**, 12 (1979).
- <sup>15</sup> J. Kortus, I. I. Mazin, K. D. Belashchenko, V. P. Antropov, and L. L. Boyer, cond-mat/0101446.

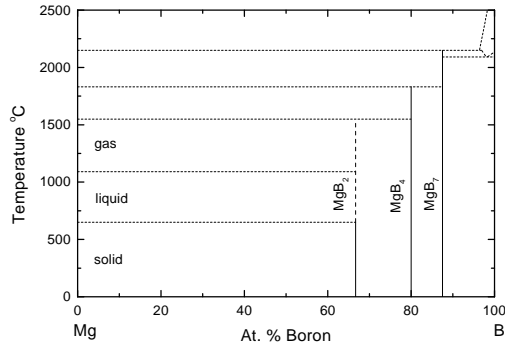


FIG. 1. Proposed, schematic, binary phase diagram for B - Mg system (After Ref. [9]).

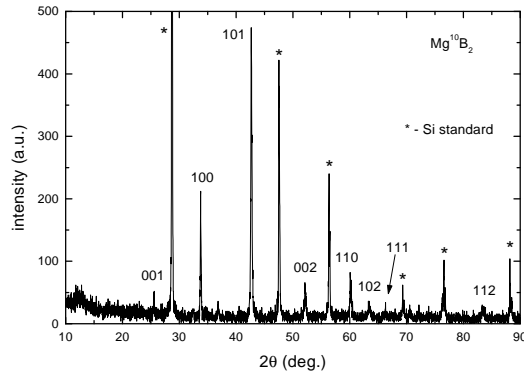


FIG. 2. Powder X-ray ( $\text{Cu K}\alpha$  radiation) diffraction spectra of  $\text{Mg}^{10}\text{B}_2$  (with h,k,l values) and Si standard (\*).

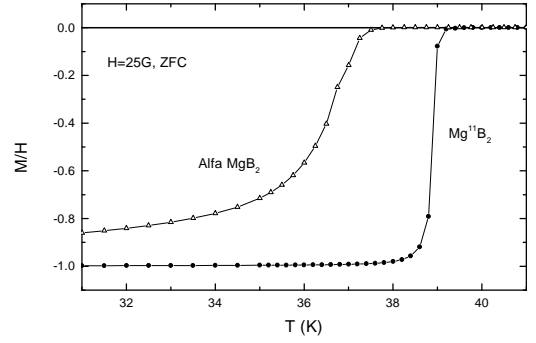


FIG. 3. Magnetization divided by applied field as a function of temperature for  $\text{Mg}^{11}\text{B}_2$  and natural boron sample of  $\text{MgB}_2$  from Alfa-Aesar. Data are normalized to 1 at 5 K, as discussed in text.

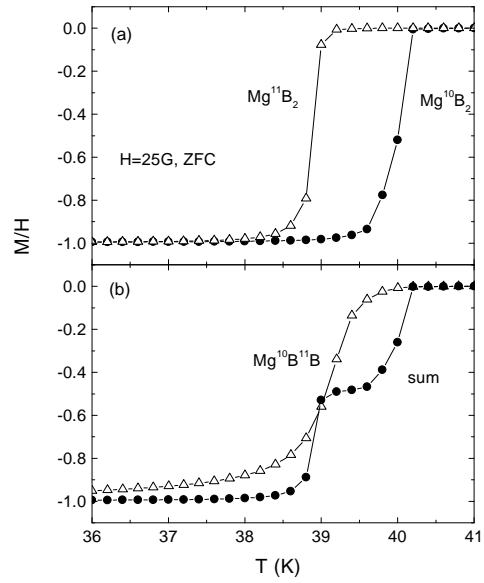


FIG. 4. (a) Magnetization divided by applied field as a function of temperature for  $\text{Mg}^{10}\text{B}_2$  and  $\text{Mg}^{11}\text{B}_2$ . (b) Magnetization divided by applied field as a function of temperature for  $\text{Mg}^{10}\text{B}^{11}\text{B}$  and sum of  $\text{Mg}^{10}\text{B}_2$  and  $\text{Mg}^{11}\text{B}_2$  data shown in panel (a). Data are normalized to  $-1$  at 5 K, as discussed in text.

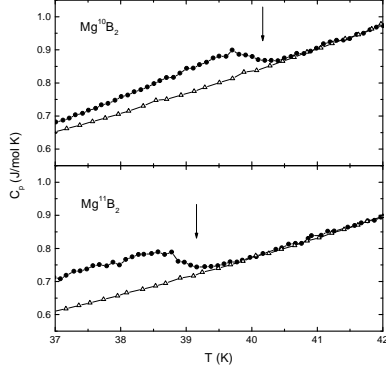


FIG. 5. Temperature dependent specific heat of  $\text{Mg}^{10}\text{B}_2$  and  $\text{Mg}^{11}\text{B}_2$  in zero (filled circles) and 90 kG (open triangles) applied field for temperatures near the  $T_c$ . Arrows mark transition temperatures determined from the magnetization measurements shown in Fig. 4a.